

## Exotic decay in cerium isotopes

K P SANTHOSH<sup>1</sup> and ANTONY JOSEPH\*

Department of Physics, Calicut University, Calicut 673 635, India

<sup>1</sup>Department of Physics, Payyanur College, Payyanur 670 327, India

\*Corresponding author

Email: ajvar@rediffmail.com

MS received 9 October 2000; revised 10 September 2001

**Abstract.** Half life for the emission of exotic clusters like  $^8\text{Be}$ ,  $^{12}\text{C}$ ,  $^{16}\text{O}$ ,  $^{20}\text{Ne}$ ,  $^{24}\text{Mg}$  and  $^{28}\text{Si}$  are computed taking Coulomb and proximity potentials as interacting barrier and many of these are found well within the present upper limit of measurement. These results lie very close to those values reported by Shanmugam *et al* using their cubic plus Yukawa plus exponential model (CYEM). It is found that  $^{12}\text{C}$  and  $^{16}\text{O}$  emissions from  $^{116}\text{Ce}$  and  $^{16}\text{O}$  from  $^{118}\text{Ce}$  are most favorable for measurement ( $T_{1/2} < 10^{10}$  s). Lowest half life time for  $^{16}\text{O}$  emission from  $^{116}\text{Ce}$  stress the role of doubly magic  $^{100}\text{Sn}$  daughter in exotic decay. Geiger–Nuttall plots were studied for different clusters and are found to be linear. Inclusion of proximity potential will not produce much deviation to linear nature of Geiger–Nuttall plots. It is observed that neutron excess in the parent nuclei slow down the exotic decay process. These findings support the earlier observations of Gupta and collaborators using their preformed cluster model (PCM).

**Keywords.** Exotic decay; cluster radioactivity; fission model; cluster model.

**PACS Nos** 23.70.+j; 23.60.+e

### 1. Introduction

Sandulescu *et al* [1] in 1980 predicted that radioactive decay process intermediate between alpha decay and spontaneous fission, commonly called exotic decay or cluster radioactivity might occur among nuclei with  $Z > 88$  on the basis of quantum mechanical fragmentation theory (QMFT) [2]. Rose and Jones [3] in 1984 first observed this type of decay experimentally in the emission of  $^{14}\text{C}$  from  $^{223}\text{Ra}$ . This discovery of cluster radioactivity renewed the interest in the study of various possible exotic decay modes of heavy nuclei. Subsequently theoretical investigations showed that this problem could be viewed in two different ways. From one side alpha decay theory has been successfully extended to incorporate heavy ion emission also [4]; from the other, cluster emission together with alpha decay have been proposed to be two different aspects of the same process, i.e. highly asymmetric fission or super asymmetric fission.

The instability against exotic cluster decay of ‘stable’ nuclei was first pointed out by Malik and collaborators [5] in 1989 and new instabilities against exotic decay of some

'stable' nuclei in the region  $Z = 50-82$  was first pointed out by Gupta *et al* in 1993 [6]. Based on preformed cluster model (PCM) Satish Kumar *et al* [7,8] and based on the analytical super asymmetric fission model (ASAFM) Poenaru *et al* [9] calculated half life time for proton rich nuclei with  $Z = 56-72$  which decays exotically. This region is interesting because the daughter nuclei in such decays are formed around the doubly magic  $^{100}\text{Sn}$  and the half lives are favorable for measurements. Moreover only  $N = Z$  clusters are emitted and  $Z/A$  values for parent, daughter and emitted cluster are nearly equal to 0.5. Experiment for producing such parent exotic nuclei were conducted at Dubna, Russia [10] and at GSI, Darmstadt, Germany [11,12].

Taking interacting potential as the sum of Coulomb and proximity potential we have calculated half life for  $^{12}\text{C}$  emission from various Ba isotopes using different mass tables [13]. The half life time predicted by us for  $^{12}\text{C}$  emission from various Ba isotopes are well within the present upper limit for measurements ( $T_{1/2} < 10^{30}$  s). In this paper we extended our studies to the exotic decay of clusters like  $^8\text{Be}$ ,  $^{12}\text{C}$ ,  $^{16}\text{O}$ ,  $^{20}\text{Ne}$ ,  $^{22}\text{Ne}$ ,  $^{24}\text{Mg}$ ,  $^{26}\text{Mg}$  and  $^{28}\text{Si}$  from different Ce isotopes.

In §2 we describe the features of Coulomb and proximity potential model and §3 contains the calculations, results and conclusion.

## 2. Coulomb and proximity potential model

The interacting potential barrier for a parent nucleus exhibiting exotic decay is given by

$$V = Z_1 Z_2 e^2 / r + V_p(z) \quad \text{for } z > 0. \quad (1)$$

Here  $Z_1$  and  $Z_2$  are atomic numbers of daughter and emitted cluster,  $r$  is the distance between the fragment centers and  $z$  is the distance between the near surface of the fragments and  $V_p$  is the proximity potential given by Blocki *et al* [14]

$$V_p(z) = 4\pi\gamma b [C_1 C_2 / (C_1 + C_2)] \phi(z/b) \quad (2)$$

with nuclear surface tension coefficient

$$\gamma = 0.9517 [1 - 1.7826(N - Z)^2 / A^2] \text{ MeV/fm}^2. \quad (3)$$

Here  $N, Z, A$  represent neutron, proton and mass number of the parent respectively.  $\phi$ , the universal proximity potential is given as [15]

$$\phi(\varepsilon) = -4.41 e^{-\varepsilon/0.7176} \quad \text{for } \varepsilon \geq 1.9475, \quad (4)$$

$$\phi(\varepsilon) = -1.7817 + 0.9270\varepsilon + 0.01696\varepsilon^2 - 0.05148\varepsilon^3 \quad \text{for } 0 \leq \varepsilon \leq 1.9475 \quad (5)$$

with  $\varepsilon = z/b$  where the width (diffuseness) of the nuclear surface  $b \approx 1$  and Siissmann central radii  $C_i$  of fragments related to sharp radii  $R_i$  is  $C_i \approx R_i - b/R_i$ . For  $R_i$  we use the semi empirical formula in terms of mass number  $A_i$  as [14]

$$R_i = 1.28A_i^{1/3} - 0.76 + 0.8A_i^{-1/3}. \quad (6)$$

For the touching configuration  $\phi(0) = -1.7817$ .

The Gamow factor  $G$  is given by

$$G = (2\pi/h) \int_{\epsilon_0}^{\epsilon_f} \sqrt{2\mu(V-Q)} dz. \quad (7)$$

Here the mass parameter is replaced by reduced mass  $\mu = mA_1A_2/A$  where  $m$  is the nucleon mass and  $A_1$  and  $A_2$  are mass numbers of daughter and emitted cluster respectively. Here  $\epsilon_0 = 2(C - C_1 - C_2)$ . At  $\epsilon_0$  potential  $V(\epsilon_0) = Q$  and  $\epsilon_f$  is defined as  $V(\epsilon_f) = Q$ , where  $Q$  is the energy released. The above integral can be evaluated numerically or analytically [16].

The barrier penetrability  $P$  is expressed as

$$P = \exp(-2G). \quad (8)$$

The half life time is given by

$$T_{1/2} = \ln 2/\lambda = \ln 2/\nu P, \quad (9)$$

where  $\nu = \omega/2\pi = 2E_v/h$ , represents number of assaults on the barrier per second and  $\lambda$ , the decay constant.  $E_v$ , the empirical zero point vibration energy is given as [17]

$$E_v = Q\{0.056 + 0.039 \exp[(4 - A_2)/2.5]\} \quad \text{for } A_2 \geq 4. \quad (10)$$

### 3. Calculation, results and conclusion

We have made our calculation taking potential energy barrier as the sum of Coulomb and proximity potential of Blocki *et al* [14,15] for touching configuration and for separated fragments. From touching configuration and down to parent central radius we use simple power law interpolation as done by Shi and Swiatecki [16]. Proximity potential was first used by Shi and Swiatecki [16] in an empirical manner and has been used quite extensively by Malik and Gupta [18] for over a decade now in preformed cluster model (PCM) which is based on the 'pocket' formula of Blocki *et al* [14]. In the present model we use another formulation of proximity potential [15]. Figures 1 and 2 represent the potential energy barrier for the emission of  $^4\text{He}$  and  $^{16}\text{O}$  respectively from  $^{116}\text{Ce}$  isotope.

Tables 1 and 2 give logarithm of predicted half life  $\log_{10}(T_{1/2})$  and other characteristics for  $^{16}\text{O}$  and  $^4\text{He}$  emission respectively from various Ce isotopes using different mass tables. We have compared our predicted half life time with those values reported by Poenaru *et al* [9] using their analytical super asymmetric fission model (ASAFM), Shanmugam *et al* [19] using their cubic plus Yukawa plus exponential model (CYEM) and Satish Kumar *et al* [8] using preformed cluster model (PCM) of Malik and Gupta [18]. It is found that our calculated values lie very close to those values reported by Shanmugam *et al* [19].

The  $^{16}\text{O}$  emission from  $^{116}\text{Ce}$  ( $Q = 31.71$  MeV,  $T_{1/2} = 1.30965 \times 10^6$  s) and from  $^{118}\text{Ce}$  (for  $Q = 29.94$  MeV,  $T_{1/2} = 2.71757 \times 10^9$  s and for  $Q = 29.97$  MeV,  $T_{1/2} = 2.33921 \times 10^9$  s) are most favorable for measurements. Out of this,  $^{16}\text{O}$  from  $^{116}\text{Ce}$  has lowest  $T_{1/2}$  value which stress the role of doubly magic daughter nuclei  $^{100}\text{Sn}$  with  $N = 50$  and  $Z = 50$  in exotic cluster decay of Ce isotopes.

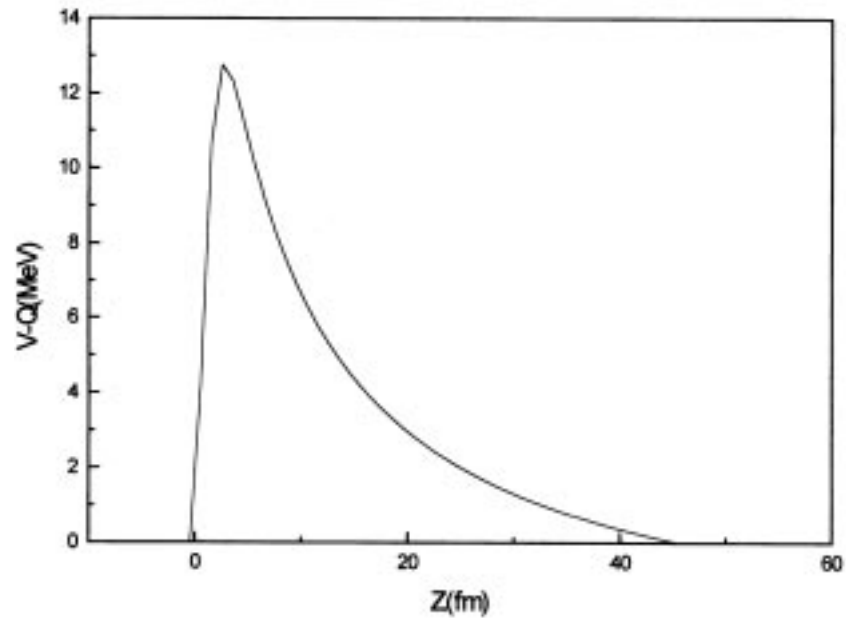


Figure 1. Potential energy barrier for the emission of  ${}^4\text{He}$  from  ${}^{116}\text{Ce}$  isotope.

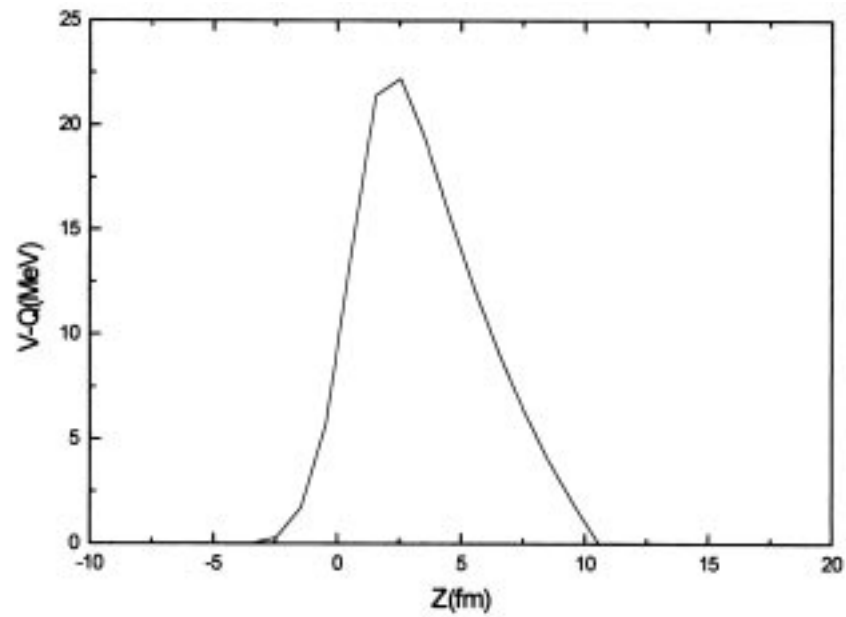


Figure 2. Potential energy barrier for the emission of  ${}^{16}\text{O}$  from  ${}^{116}\text{Ce}$  isotope.

**Table 1.** Logarithm of predicted half life time and other characteristics of  $^{16}\text{O}$  emission from various Ce isotopes using different mass tables.  $Q$  values are taken from [20].

Parent nuclei	Emitted cluster	Daughter nuclei	$Q$ value (MeV)	Penetrability $P$	Decay constant $\lambda$	Calculated $\log_{10} T_{1/2}$			
						Present	CYEM [19]	ASAFM [9]	PCM [8]
$^{116}\text{Ce}$	$^{16}\text{O}$	$^{100}\text{Sn}$	31.71 <sup>a</sup>	6.12654E-28	5.292E-07	6.12			6.14
$^{118}\text{Ce}$	$^{16}\text{O}$	$^{102}\text{Sn}$	29.94 <sup>a</sup>	3.12705E-31	2.551E-10	9.43			10.79
			29.26	1.01470E-32	8.087E-12	10.93	10.97	11.90	
			27.97	1.13475E-35	8.645E-15	13.90	13.74	14.50	
			29.97	3.62921E-31	2.963E-10	9.37	9.51	10.60	
			29.08	4.02489E-33	3.188E-12	11.34	11.34	12.30	
			29.75	1.21218E-31	9.823E-11	9.85	9.96	11.00	
$^{120}\text{Ce}$	$^{16}\text{O}$	$^{104}\text{Sn}$	27.12 <sup>a</sup>	2.30664E-37	1.704E-16	15.61			16.79
			27.73	6.90985E-36	5.219E-15	14.12	14.05	14.80	
			26.88	5.88827E-38	4.311E-17	16.21	16.00	16.60	
			25.02	8.34774E-43	5.689E-22	21.09	20.60	20.80	
			27.19	3.42476E-37	2.536E-16	15.44	15.28	15.90	
			26.57	9.85291E-39	7.131E-18	16.99	16.74	17.30	
			26.87	5.56068E-38	4.069E-17	16.23	16.03	16.60	
$^{121}\text{Ce}$	$^{16}\text{O}$	$^{105}\text{Sn}$	26.16	1.29644E-39	9.238E-19	17.88	17.62	19.70	
			25.48	2.13035E-41	1.478E-20	19.67	19.31	21.30	
			25.61	4.72578E-41	3.296E-20	19.32	18.99	21.00	
			27.48	2.54666E-36	1.906E-15	14.56	14.51	16.90	
			25.12	2.27876E-42	1.559E-21	20.65	20.24	22.20	
			25.51	2.56161E-41	1.780E-20	19.59	19.24	21.20	
$^{122}\text{Ce}$	$^{16}\text{O}$	$^{106}\text{Sn}$	24.69 <sup>a</sup>	2.13691E-43	1.437E-22	21.68			28.07
			25.13	3.48409E-42	2.385E-21	20.46	20.11	20.40	
			24.44	4.24473E-44	2.826E-23	22.39	21.93	22.10	
			24.73	2.76185E-43	1.860E-22	21.57	21.16	21.40	
			23.96	1.78793E-45	1.167E-24	23.77	23.25	23.30	
			24.52	7.13718E-44	4.767E-23	22.16	21.72	21.90	
$^{123}\text{Ce}$	$^{16}\text{O}$	$^{107}\text{Sn}$	23.61	2.36815E-46	1.523E-25	24.66	24.13	25.80	
			23.03	4.21602E-48	2.645E-27	26.42	25.81	27.40	
			23.20	1.39287E-47	8.802E-27	25.90	25.31	26.90	
			22.71	4.30003E-49	2.660E-28	27.42	26.76	28.30	
			23.22	1.60187E-47	1.013E-26	25.84	25.25	26.90	
$^{124}\text{Ce}$	$^{16}\text{O}$	$^{108}\text{Sn}$	22.26 <sup>a</sup>	2.22455E-50	1.349E-29	28.71			37.39
			22.59	2.50263E-49	1.540E-28	27.65	27.02	26.90	
			21.89	1.38886E-51	8.281E-31	29.92	29.19	28.90	
			22.31	3.22026E-50	1.957E-29	28.55	27.88	27.70	
			21.58	1.29239E-52	7.596E-32	30.96	30.18	29.80	
			22.22	1.65334E-50	1.001E-29	28.84	28.16	27.90	

<sup>a</sup> $Q$  values are taken from [8].

**Table 2.** Logarithm of predicted half life time and other characteristics of  $^4\text{He}$  emission from various Ce isotopes using different mass tables.  $Q$  values are taken from [20].

Parent nuclei	Emitted cluster	Daughter nuclei	$Q$ value (MeV)	Penetrability $P$	Decay constant $\lambda$	Calculated $\log_{10} T_{1/2}$			
						Present	CYEM [19]	ASAFM [9]	PCM [8]
$^{116}\text{Ce}$	$^4\text{He}$	$^{112}\text{Ba}$	3.09 <sup>a</sup>	2.94866E-29	4.186E-09	8.219			6.15
$^{118}\text{Ce}$	$^4\text{He}$	$^{114}\text{Ba}$	2.58 <sup>a</sup>	2.84922E-34	3.377E-14	13.31			11.04
			3.18	2.48935E-28	3.637E-08	7.28	7.25	6.60	
			1.48	3.48632E-53	2.371E-33	32.47	32.16	31.20	
			3.40	1.37099E-26	2.141E-06	5.51	5.49	5.00	
			3.57	2.32192E-25	3.808E-05	4.26	4.24	3.80	
$^{120}\text{Ce}$	$^4\text{He}$	$^{116}\text{Ba}$	2.46	1.07345E-35	1.213E-15	14.76	14.58	13.70	
			2.33 <sup>a</sup>	2.77794E-37	2.974E-17	16.37			12.98
			3.16	1.69366E-28	2.459E-08	7.45	7.35	6.80	
			2.71	9.29767E-33	1.158E-12	11.78	11.64	11.00	
			1.21	2.30783E-61	1.283E-41	40.73	40.39	39.20	
			2.60	5.76347E-34	6.885E-14	13.00	12.86	12.30	
$^{121}\text{Ce}$	$^4\text{He}$	$^{117}\text{Ba}$	2.57	2.67839E-34	3.092E-14	13.35	13.20	12.50	
			2.26	3.07880E-38	3.197E-18	17.34	17.15	16.40	
			2.91	1.07187E-30	1.433E-10	9.68	9.58	9.40	
			2.24	1.75322E-38	1.804E-18	17.58	17.40	17.20	
			2.37	1.01686E-36	1.107E-16	15.80	15.63	15.50	
			4.24	2.95902E-21	5.764E-01	0.08	-0.02	0.10	
$^{122}\text{Ce}$	$^4\text{He}$	$^{118}\text{Ba}$	1.88	2.75865E-44	2.383E-24	23.46	23.24	23.10	
			2.26	3.34953E-38	3.478E-18	17.30	17.12	16.80	
			2.09 <sup>a</sup>	1.10523E-40	1.061E-20	19.81			14.74
			2.87	4.78737E-31	6.312E-11	10.04	9.94	9.50	
			2.18	2.58513E-39	2.589E-19	18.43	18.25	17.70	
			2.46	1.51690E-35	1.714E-15	14.61	14.46	13.80	
$^{123}\text{Ce}$	$^4\text{He}$	$^{119}\text{Ba}$	1.70	8.04444E-48	6.283E-28	27.04	26.80	26.20	
			2.26	3.63247E-38	3.772E-18	17.26	17.09	16.50	
			2.43	6.96022E-36	7.770E-16	14.95	14.80	14.60	
			1.86	1.37411E-44	1.174E-24	23.77	23.56	23.50	
			2.03	1.30122E-41	1.214E-21	20.76	20.56	20.50	
			1.54	1.79278E-51	1.268E-31	30.74	30.48	30.50	
$^{124}\text{Ce}$	$^4\text{He}$	$^{120}\text{Ba}$	2.04	1.89568E-41	1.777E-21	20.59	20.40	20.20	
			1.73 <sup>a</sup>	4.01922E-47	3.195E-27	26.34			21.48
			2.40	3.13356E-36	3.455E-16	15.30	15.16	14.70	
			1.70	9.34546E-48	7.299E-28	26.98	26.75	26.20	
			2.12	3.76460E-40	3.667E-20	19.28	19.10	18.60	
			1.38	9.47770E-56	6.009E-36	35.06	34.78	34.00	
			2.02	9.59652E-42	9.806E-22	20.89	20.70	20.10	

<sup>a</sup> $Q$  values are taken from [8].

In table 3, Cal. I gives logarithm of predicted half life time  $\log_{10}(T_{1/2})$  value for different clusters like  $^8\text{Be}$ ,  $^{12}\text{C}$ ,  $^{20}\text{Ne}$ ,  $^{22}\text{Ne}$ ,  $^{24}\text{Mg}$ ,  $^{26}\text{Mg}$  and  $^{28}\text{Si}$ . Most of them are well within the present upper limit of measurements. Here  $^{12}\text{C}$  emission from  $^{116}\text{Ce}$  (for  $Q = 21.17$  MeV,  $T_{1/2} = 9.94412 \times 10^6$  s) is the most favorable for measurement.

**Table 3.** Logarithm of predicted half life time and other characteristics for  $^8\text{Be}$ ,  $^{12}\text{C}$ ,  $^{20}\text{Ne}$ ,  $^{22}\text{Ne}$ ,  $^{24}\text{Mg}$ ,  $^{26}\text{Mg}$  and  $^{28}\text{Si}$  emissions from various Ce isotopes and their comparison with PCM.  $Q$  values are taken from [8].

Parent nuclei	Emitted cluster	Daughter nuclei	$Q$ value (MeV)	Penetrability $P$	Decay constant $\lambda$	$\log_{10} T_{1/2}$		
						Present Cal. I	Present Cal. II	PCM [8]
$^{116}\text{Ce}$	$^8\text{Be}$	$^{108}\text{Xe}$	7.32	2.74101E-47	6.198E-27	26.05	25.68	23.52
$^{118}\text{Ce}$	$^8\text{Be}$	$^{110}\text{Xe}$	5.61	1.35520E-60	2.348E-40	39.47	39.07	35.48
$^{120}\text{Ce}$	$^8\text{Be}$	$^{112}\text{Xe}$	4.55	2.39877E-72	3.371E-52	51.31	50.94	49.01
$^{122}\text{Ce}$	$^8\text{Be}$	$^{114}\text{Xe}$	3.89	5.86879E-82	7.052E-62	60.99	60.66	55.36
$^{124}\text{Ce}$	$^8\text{Be}$	$^{116}\text{Xe}$	3.17	9.19393E-96	9.002E-76	74.89	74.57	66.03
$^{116}\text{Ce}$	$^{12}\text{C}$	$^{104}\text{Te}$	21.17	1.18197E-28	6.969E-08	6.998	7.214	6.20
$^{118}\text{Ce}$	$^{12}\text{C}$	$^{106}\text{Te}$	17.46	1.29786E-38	6.311E-18	17.04	17.06	16.47
$^{120}\text{Ce}$	$^{12}\text{C}$	$^{108}\text{Te}$	15.19	2.83273E-46	1.198E-25	24.76	24.78	25.08
$^{122}\text{Ce}$	$^{12}\text{C}$	$^{110}\text{Te}$	14.80	1.41766E-47	5.844E-27	26.07	26.28	30.57
$^{124}\text{Ce}$	$^{12}\text{C}$	$^{112}\text{Te}$	12.77	2.13625E-56	7.598E-36	34.96	35.19	40.77
$^{116}\text{Ce}$	$^{20}\text{Ne}$	$^{96}\text{Cd}$	34.76	8.04943E-42	7.586E-21	19.96	19.47	19.68
$^{118}\text{Ce}$	$^{20}\text{Ne}$	$^{98}\text{Cd}$	34.48	5.58809E-42	5.224E-21	20.12	20.06	22.36
$^{120}\text{Ce}$	$^{20}\text{Ne}$	$^{100}\text{Cd}$	32.50	2.87741E-46	2.536E-25	24.44	24.46	26.82
$^{122}\text{Ce}$	$^{20}\text{Ne}$	$^{102}\text{Cd}$	28.58	1.82296E-56	1.413E-35	34.69	34.48	41.15
$^{124}\text{Ce}$	$^{20}\text{Ne}$	$^{104}\text{Cd}$	26.53	1.78461E-62	1.284E-41	40.73	40.58	50.11
$^{122}\text{Ce}$	$^{22}\text{Ne}$	$^{100}\text{Cd}$	26.38	3.07499E-64	2.198E-43	42.50	41.06	49.98
$^{124}\text{Ce}$	$^{22}\text{Ne}$	$^{102}\text{Cd}$	26.10	7.51923E-65	5.318E-44	43.12	41.95	53.86
$^{116}\text{Ce}$	$^{24}\text{Mg}$	$^{92}\text{Pd}$	41.16	1.00526E-46	1.121E-25	24.79	23.99	25.81
$^{118}\text{Ce}$	$^{24}\text{Mg}$	$^{94}\text{Pd}$	41.53	2.48944E-45	2.801E-24	23.39	23.26	26.39
$^{120}\text{Ce}$	$^{24}\text{Mg}$	$^{96}\text{Pd}$	40.87	2.96583E-46	3.283E-25	24.32	24.56	26.50
$^{122}\text{Ce}$	$^{24}\text{Mg}$	$^{98}\text{Pd}$	37.73	3.74020E-53	3.823E-32	31.26	31.21	40.43
$^{124}\text{Ce}$	$^{24}\text{Mg}$	$^{100}\text{Pd}$	34.65	8.83675E-61	8.294E-40	38.92	38.59	45.89
$^{122}\text{Ce}$	$^{26}\text{Mg}$	$^{96}\text{Pd}$	34.89	5.74934E-61	5.433E-40	39.11	37.98	46.79
$^{124}\text{Ce}$	$^{26}\text{Mg}$	$^{98}\text{Pd}$	33.01	4.63836E-66	4.147E-45	44.22	42.94	46.95
$^{116}\text{Ce}$	$^{28}\text{Si}$	$^{88}\text{Ru}$	48.26	2.41571E-48	3.157E-27	26.34	25.71	27.68
$^{118}\text{Ce}$	$^{28}\text{Si}$	$^{90}\text{Ru}$	48.18	7.89775E-48	1.031E-26	25.83	25.85	28.50
$^{120}\text{Ce}$	$^{28}\text{Si}$	$^{92}\text{Ru}$	48.10	2.29684E-47	2.992E-26	25.37	25.99	27.50
$^{122}\text{Ce}$	$^{28}\text{Si}$	$^{94}\text{Ru}$	46.56	4.10641E-50	5.178E-29	28.13	28.79	37.28
$^{124}\text{Ce}$	$^{28}\text{Si}$	$^{96}\text{Ru}$	43.06	1.08941E-57	1.270E-36	35.74	35.69	41.69

Figure 3 gives Geiger–Nuttall plots for  $\log_{10}(T_{1/2})$  vs.  $Q^{-1/2}$  for different clusters from various Ce isotopes. Geiger–Nuttall plots for all clusters are found to be linear with different slopes and intercepts. From the observed linear nature of these plots, we arrived at an equation for logarithm of half life time as

$$\log_{10}(T_{1/2}) = \frac{X}{\sqrt{Q}} + Y. \quad (11)$$

The values of slope  $X$  and intercept  $Y$  for different clusters are given in table 4. Using the above equation we have calculated half life time for all clusters from various Ce isotopes and are in good agreement with theoretical values.

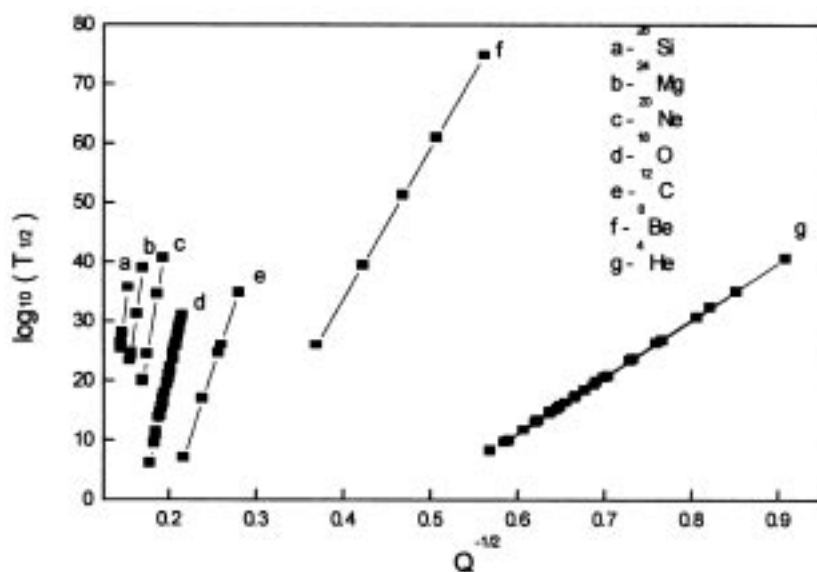


**Figure 3.** Geiger–Nuttall plot of  $\log_{10}(T_{1/2})$  vs.  $Q^{-1/2}$  for various cluster emission from different Ce isotopes.

**Table 4.** Slope and intercept values of Geiger–Nuttall plots for different clusters emitted from various Ce isotopes.

Emitted cluster	Slope X	Intercept Y
${}^4\text{He}$	95.79888	-46.43929
${}^8\text{Be}$	254.20336	-67.87994
${}^{12}\text{C}$	446.96278	-90.04361
${}^{16}\text{O}$	659.11292	-110.94215
${}^{20}\text{Ne}$	857.25478	-125.71802
${}^{24}\text{Mg}$	1043.9027	-138.51576
${}^{28}\text{Si}$	1181.4194	-144.47783

From the observed variation of slope and intercept of Geiger–Nuttall plots with proton number ( $Z_2$ ) of the emitted cluster we have arrived at a general equation for half life time which are applicable to all clusters from various Ce isotopes as

$$\log_{10}(T_{1/2}) = \frac{X(Z_2)}{\sqrt{Q}} + Y(Z_2), \tag{12}$$

where

$$X(Z_2) = -0.39712(Z_2)^3 + 9.04574(Z_2)^2 + 36.32311Z_2 - 10.14493, \tag{13}$$

$$Y(Z_2) = 0.02872(Z_2)^3 - 0.28315(Z_2)^2 - 10.20002Z_2 - 24.9127. \tag{14}$$



Using the above equation we have calculated half life time for all possible cluster emission from various Ce isotopes and are given in table 3 as Cal. II. These values are also compared with theory and also with other models.

Figures 4 and 5 give Geiger–Nuttall plots of  $\log_{10}(T_{1/2})$  vs.  $-\ln P$  for different clusters from various Ce isotopes. These are also found to be straight lines with nearly equal slopes and intercepts. This indicates that the inclusion of proximity potential does not produce significant deviation to the linear nature of Geiger–Nuttall plots.

We have taken cluster formation probability as unity for all clusters irrespective of their masses. So present model differ from the preformed cluster model (PCM) by a factor  $P_0$ , the cluster formation probability. But we have included the contribution of overlap region ( $\epsilon_0 < \epsilon < 0$ ) in barrier penetrability calculation. This is the reason for identical  $\log_{10}(T_{1/2})$  value with that of PCM. [For e.g., in the case of  $^{16}\text{O}$  decay from  $^{116}\text{Ce}$ , present=6.12 and PCM=6.14.] In the present model  $z = 0$  refers the touching configuration and as  $z$  decreases from 0 to  $\epsilon_0$  the two fragments get fused. So the factor 2 in  $\epsilon_0$  represents the diameter of the parent and fusing fragments. Also at  $\epsilon_0$  the potential  $V(\epsilon_0) = Q$ .

When the half life time for different clusters from  $^{116}\text{Ce}$  are compared with that from other heavier Ce isotopes up to  $^{124}\text{Ce}$ , the  $\log_{10}(T_{1/2})$  values are found to increase. For example, the  $\log_{10}(T_{1/2})$  value for  $^{16}\text{O}$  increases from 6.12 s (for  $^{116}\text{Ce}$ ,  $Q = 31.71$  MeV) to 27.65 s (for  $^{124}\text{Ce}$ ,  $Q = 22.59$  MeV). All these cases refer to doubly magic or near doubly magic daughter Sn nuclei. From this it is clear that the presence of neutron excess in parent nuclei will slow down the exotic decay process.

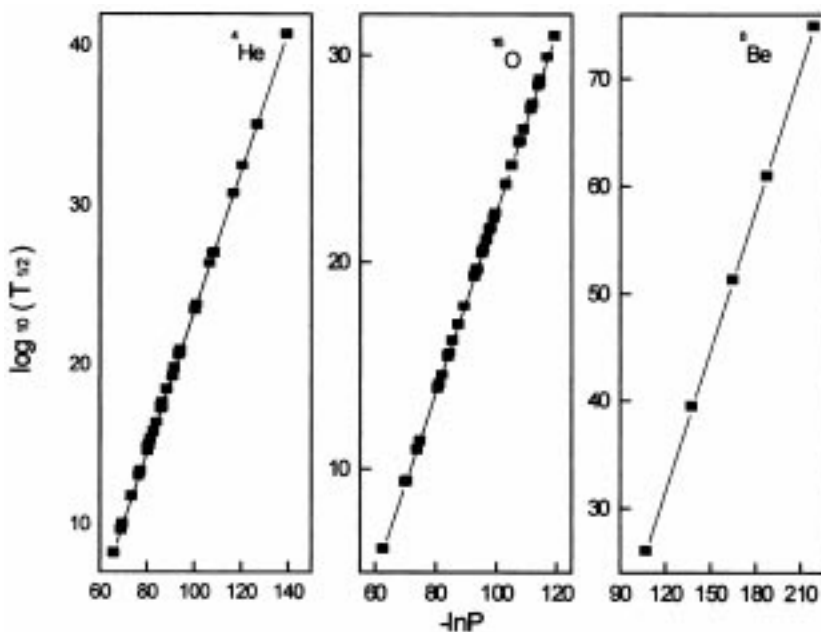


**Figure 4.** Geiger–Nuttall plot of  $\log_{10}(T_{1/2})$  vs.  $-\ln P$  for  $^4\text{He}$ ,  $^{16}\text{O}$  and  $^8\text{Be}$  from various Ce isotopes.

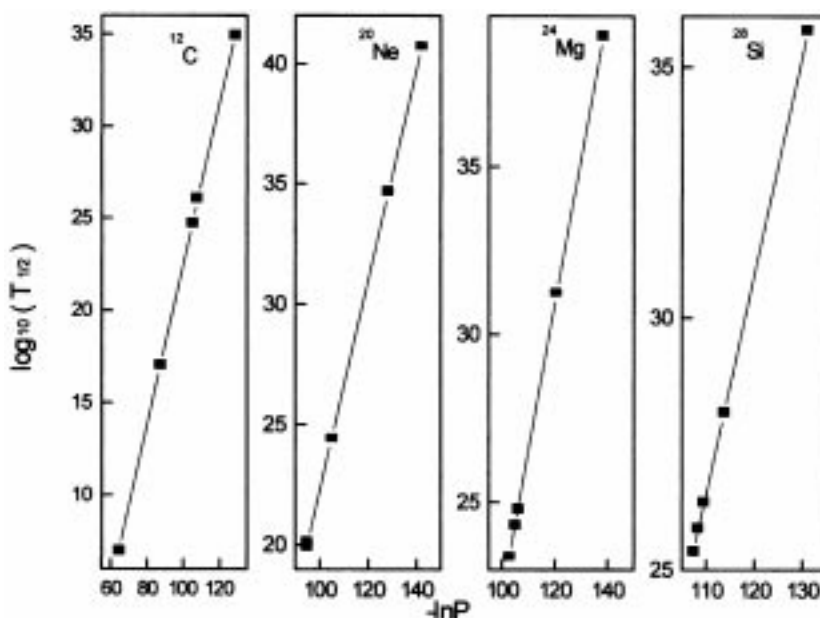


**Figure 5.** Geiger–Nuttall plot of  $\log_{10}(T_{1/2})$  vs.  $-\ln P$  for  $^{12}\text{C}$ ,  $^{20}\text{Ne}$ ,  $^{24}\text{Mg}$  and  $^{28}\text{Si}$  from various Ce isotopes.

When emission of  $^{22}\text{Ne}$  and  $^{20}\text{Ne}$  from the same parent (either  $^{122}\text{Ce}$  or  $^{124}\text{Ce}$ ) are compared, it is found that  $^{20}\text{Ne}$  has the lowest  $T_{1/2}$  value. Also when emission of  $^{26}\text{Mg}$  and  $^{24}\text{Mg}$  from the same parent (either  $^{122}\text{Ce}$  or  $^{124}\text{Ce}$ ) are compared, it is found that  $^{24}\text{Mg}$  has the lowest  $T_{1/2}$  value. This points to the fact that clusters with  $N = Z$  are most probable for decay.

The role of  $^{100}\text{Sn}$  in exotic decay process, no effect of proximity potential on Geiger–Nuttall plots and role of neutron excess in parent nuclei were first pointed out by Satish Kumar *et al* [7,8,21]. So our findings support earlier observations of Gupta and collaborators using preformed cluster model (PCM).

### Acknowledgement

One of the authors (KPS) is grateful to the University Grants Commission, New Delhi for financial support under FIP (IX Plan).

### References

- [1] A Sandulescu, D N Poenaru and W Greiner, *Fiz. Elem. Chastits At. Yadra* II, 1334 (1980) [*Sov. J. Part. Nucl.* II, 528 (1980)]
- [2] R K Gupta, in *Heavy elements and related new phenomena* edited by R K Gupta and W Greiner (World Scientific Pub., Singapore, 1999) vol II, p. 730

- [3] H J Rose and G A Jones, *Nature (London)* **307**, 245 (1984)
- [4] R Blendowske, T Fliessbach and H Walliser, *Z. Phys.* **A339**, 121 (1991)
- [5] S S Malik, S Singh, R K Puri, S Kumar and R K Gupta, *Pramana – J. Phys.* **32**, 419 (1989)
- [6] R K Gupta, S Singh, R K Puri and W Scheid, *Phys. Rev.* **C47**, 561 (1993)
- [7] S Kumar and R K Gupta, *Phys. Rev.* **C49**, 1922 (1994)
- [8] S Kumar, D Bir and R K Gupta, *Phys. Rev.* **C51**, 1762 (1995)
- [9] D N Poenaru, W Greiner and R Gherghescu, *Phys. Rev.* **C47**, 2030 (1993)
- [10] Yu Ts Oganessian, V L Mikheev and S P Tretyakova, Report No. E7-93-57 (JINR, Dubna, 1993)
- [11] A Guglielmetti, R Bonetti, G Poli, P B Price, A J Westphal, Z Janas, H Keller, R Kirchner, O Klepper, A Piechaczek, E Roeckl, K Schmidt, A Plochocki, J Szerypo and B Blank, *Phys. Rev.* **C52**, 740 (1995)
- [12] A Guglielmetti, B Blank, R Bonetti, Z Janas, H Keller, R Kirchner, O Klepper, A Piechaczek, A Plochocki, G Poli, P B Price, E Roeckl, K Schmidt, J Szerypo and A J Westphal, *Nucl. Phys.* **A583**, 867c (1995)
- [13] K P Santhosh and Antony Joseph, *Pramana – J. Phys.* **55**, 375 (2000)
- [14] J Blocki, J Randrup, W J Swiatecki and C F Tsang, *Ann. Phys. (N.Y.)* **105**, 427 (1977)
- [15] J Blocki and W J Swiatecki, *Ann. Phys. (N.Y.)* **132**, 53 (1981)
- [16] Y J Shi and W J Swiatecki, *Nucl. Phys.* **A438**, 450 (1985)
- [17] D N Poenaru, M Ivascu, A Sandulescu and W Greiner, *Phys. Rev.* **C32**, 572 (1985)
- [18] S S Malik and R K Gupta, *Phys. Rev.* **C39**, 1992 (1989)
- [19] G Shanmugam, G M Carmel, Vigila Bai and B Kamalaharan, *Phys. Rev.* **C51**, 2616 (1995)
- [20] D N Poenaru, D Schnabel, W Greiner, D Mazilu and I Cata, Report No. GSI-90-28, 1990.
- [21] S Kumar, J S Batra and R K Gupta, *J. Phys. G: Nucl. Part. Phys.* **22**, 215 (1996)